Neutron Stars as Continuous Gravitational Wave Sources: Status and Perspectives

Compact Stars in the QCD phase diagram (CSQCD2026)

19 May 2026

Ornella Juliana Piccinni

Universitat de les Illes Balears

The Gravitational Wave Spectrum
Sources
Detectors
Big Bang
Supermassive Black Hole Binary Merger
Compact Binary Inspiral & Merger
Extreme Mass-Ratio Inspirals
Pulsars, Supernovae
Wave Period
age of the universe
years
hours
seconds
milliseconds
10^{-16}
10^{-14}
10^{-12}
10^{-10}
10^{-8}
10^{-6}
10^{-4}
10^{-2}
1
10^{2}
Wave Frequency
CMB Polarization
Radio Pulsar Timing Arrays
Space-based interferometers
Terrestrial interferometers
David Champion


compact binary inspiral
continuous
MODELLED
SHORT DURATION
LONG DURATION
UNMODELLED
burst
stochastic
@astronerdika
Credit: Shanika Galaudage / OzGrav

Observing scenarios

Some CW review: Piccinni, Galaxies, 10(3) (2022);
Riles, Living Reviews in Relativity 26, 3 (2023);
Wette, Astroparticle Physics 153 (2023) 102880

Persistent signal (long-lived): Produced by a nearly periodic mass quadrupole moment variation

- Very hot **newborn NSs** (including magnetars), right after the formation, i.e., after the merger or core-collapse supernova having high spin-down rates
- **'Young' NSs** such as stable supernova remnants during the initial spin-down phase
- Fast-spinning pulsars, i.e., **old stable millisecond pulsars** with small spin-down
- **Accreting low mass X-ray binaries** (LMXBs) emitting thermal X-ray radiation and characterized by spin-wandering
- **Glitching pulsars**, likely associated with interior superfluid effects.

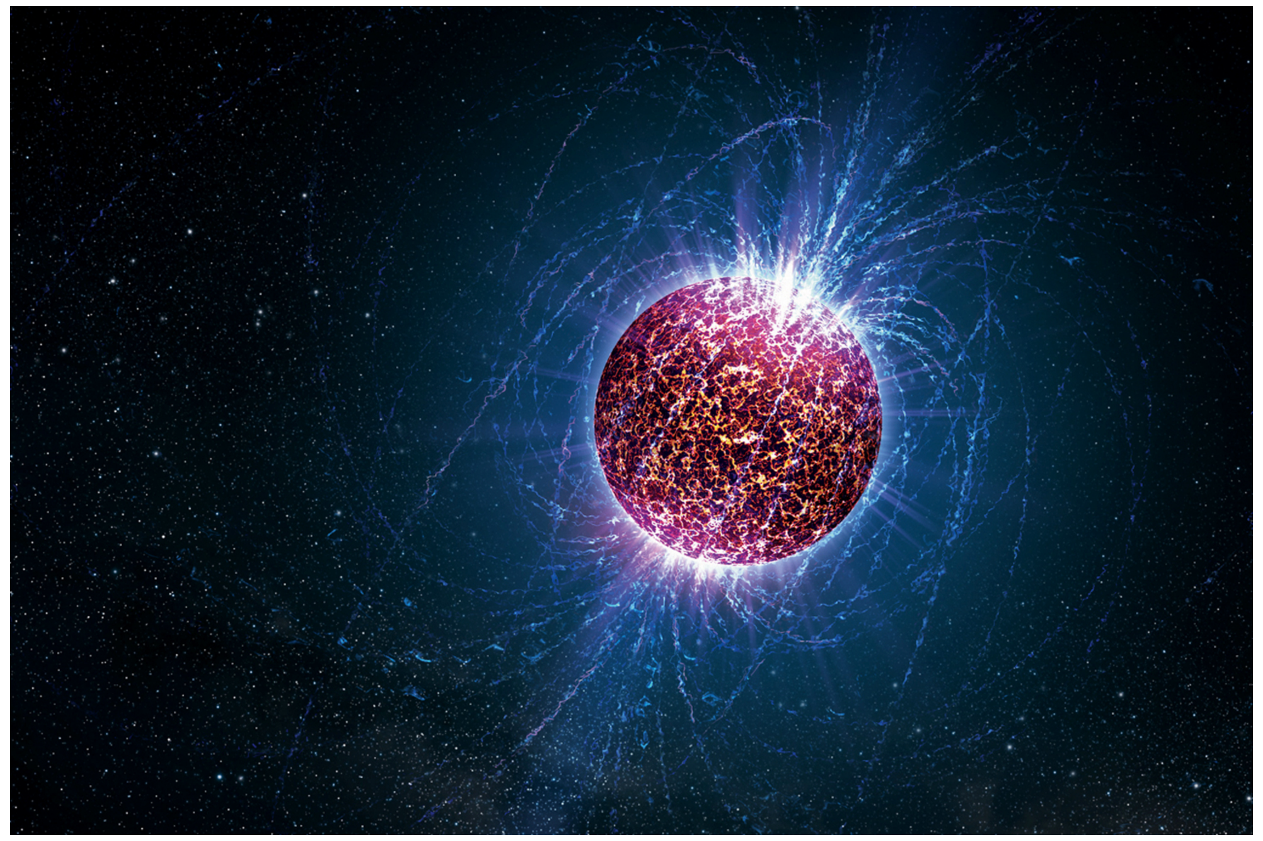

Credit: C. Reed, Penn State/Mc Gill University

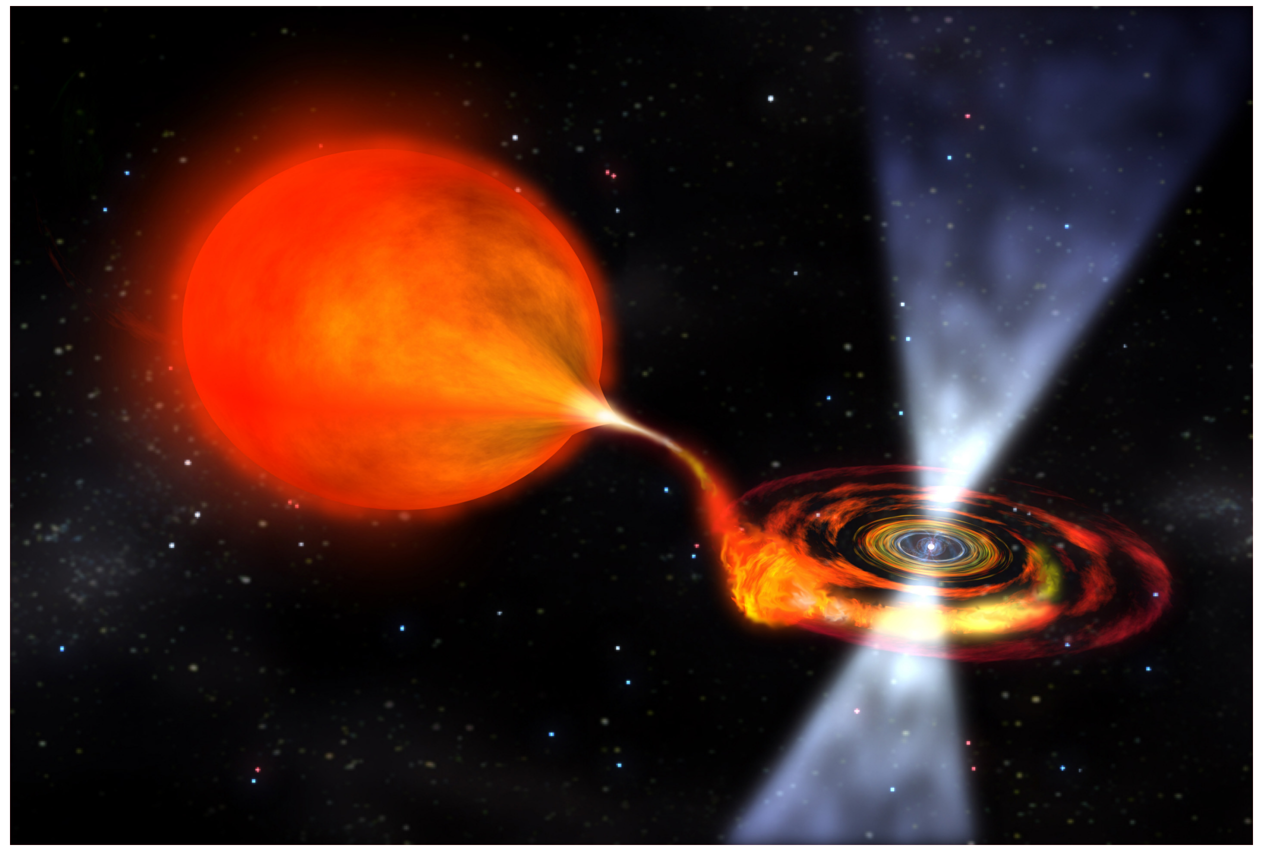

Most of these sources are detectable in the Milky Way or the local group of galaxies (i.e. kpc to at most a few Mpc)

GW emission mechanisms:

1. Ellipticity
2. R-modes

Ellipticity

non-precessing, rotating around one of the axes

$$h_0 \cong 10^{-27}\left(\frac{I_3}{10^{38}\ \mathrm{kg\,m^2}}\right)\left(\frac{10\,\mathrm{kpc}}{d}\right)\left(\frac{f}{100\ \mathrm{Hz}}\right)^2\left(\frac{\epsilon}{10^{-6}}\right) \ll h_{0_{CBC}}$$

$$h_0 = \frac{4\pi^2 G}{c^4}\frac{I_3 f^2}{d}\epsilon$$

I_3: moment of inertia

ϵ: ellipticity

$$\epsilon = \left|\frac{I_1 - I_2}{I_3}\right|$$

deformation due to:

1. elastic stresses
2. magnetic field

here $f = 2f_\star$

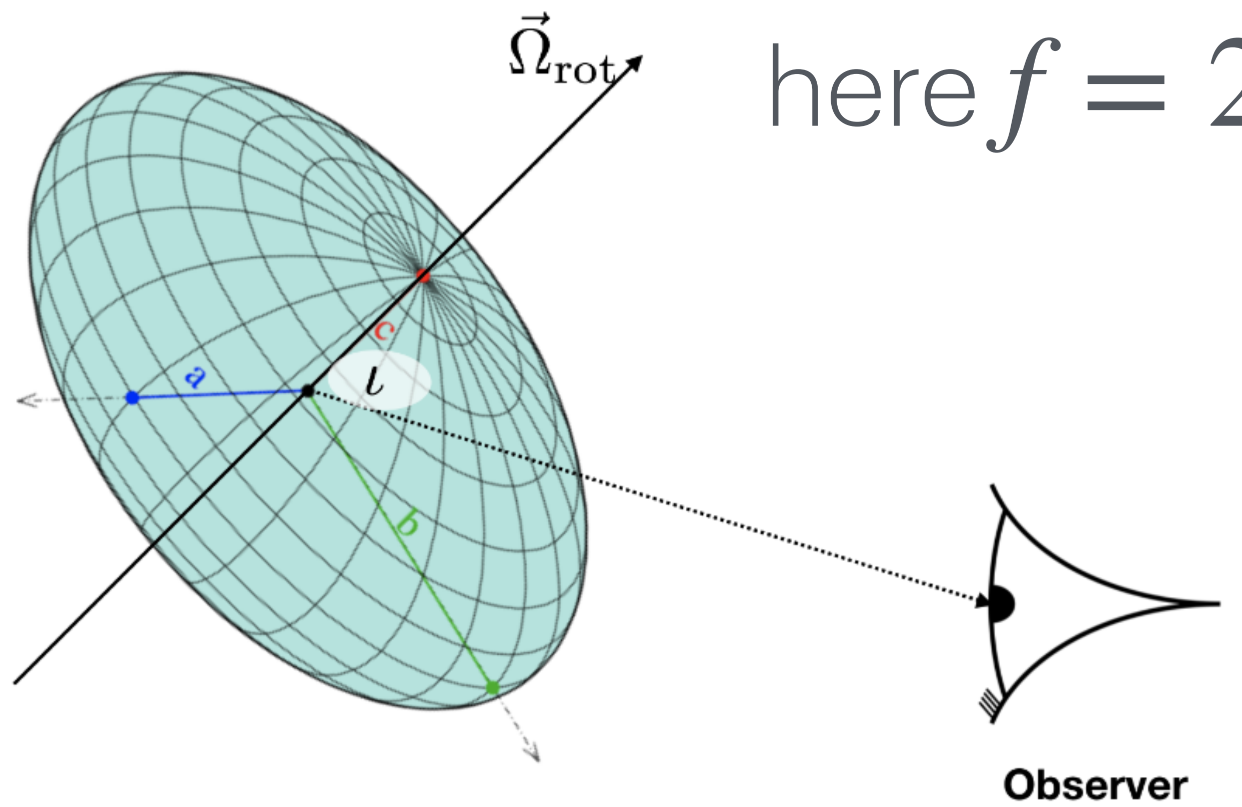

Credit: S. Mastrogiovanni

What is the actual value of ϵ?

How can we determine if the ellipticity is caused by magnetic fields or by elastic stresses?

$\epsilon_{max} < 10^{-6}\left(\frac{b}{10^{-5}}\right)\left(\frac{u_{break}}{0.1}\right)$ crustal strain $\quad \epsilon \approx 10^{-9}\left(\frac{B}{10^{12}\ \mathrm{G}}\right)$ magnetic field (Superconducting cores)

N. Andersson et al. 2011

Jones&Riles arXiv:2403.02066, Jones, CQG 19, 1255 (2002)

Estimates on the ellipticity

For isolated NS the maximum foreseen ellipticity depends on the star crust physics, the matter equation of state at supra-nuclear density and on the deformation mechanism.

Theoretical models K. Glampedakis & L. Gualtieri [Astro. and Space Science Lib., vol 457. Springer, 2018]

- **Solid strange stars**: $\epsilon \leq 6 \times 10^{-4}$
- **Hybrid and meson condensates stars**: $\epsilon \leq 3 - 9 \times 10^{-6}$
- **Canonical magnetic deformations:** $\epsilon \leq 2 - 7 \times 10^{-7}$
- **Buried magnetic field in MSPs:** $\epsilon_{fid} \sim 10^{-9}$ and a buried magnetic field of 10^{11} G Woan+[ApJL,863:L40, 2018]

Above models more stringent than older results Johnson-McDaniel+ [PRD 88, 044004 (2013)]

- **normal NS matter**: $\epsilon \leq 10^{-5}$
- **hybrid stars:** $\epsilon \leq 10^{-3}$
- **extreme quark stars:** $\epsilon \leq 10^{-1}$

Larger ellipticity may occur if the true EoS of dense matter allows for exotic phases of matter in the core (e.g. CFL/2SC)

R-modes

- Inertial modes restored by Coriolis force in a *rotating star*: ***r-modes***

Whether an r-mode grows or decays depends on the competition between these 2 effects:

- GW driving (stronger at high spin frequency), ***GW emission amplifies*** this oscillation (CFS instability)
- various ***damping mechanisms*** (shear/bulk viscosity in the fluid, boundary layer friction at the crust–core interface, effects of superfluidity, hyperons, quarks, etc.).
- no consensus on the exact shape of the ***r-mode instability window in (f,T),*** different microphysics assumptions give very different curves.
- If unstable r-modes reach large amplitude, **young fast NSs** can spin down rapidly and emit strong but evolving CWs.
- If amplitudes saturate at low values, r-modes may still operate in **LMXBs and millisecond pulsars**, producing weaker CWs that are prime targets for directed/targeted searches.

GW frequency

see also Jones 2021 arXiv:2111.08561

non-axisymetries in rigid rotating bodies (i.e. mountains)

$f = 2f_\star, \quad \theta = 0$

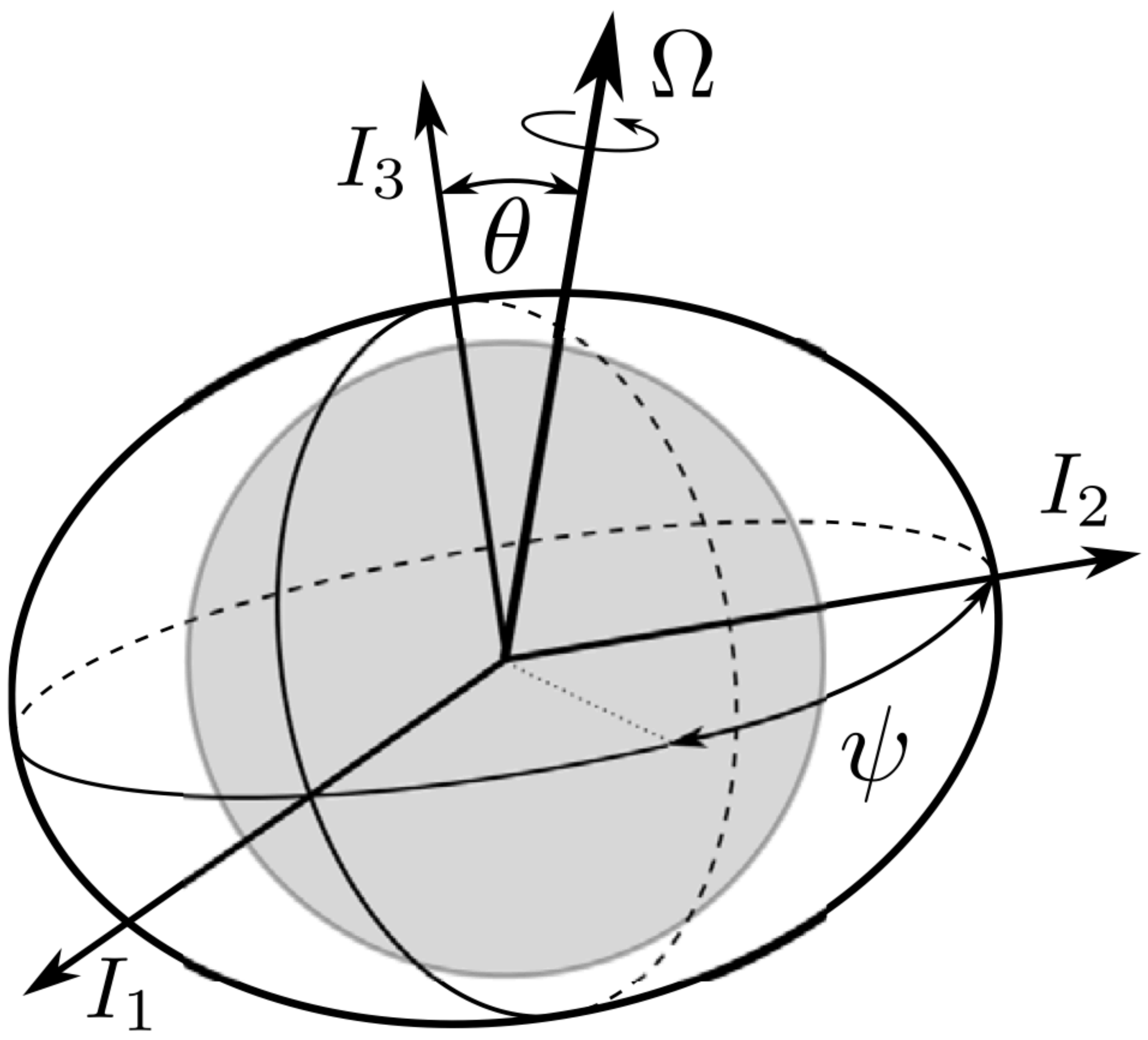

M. Bejger and A. Królak 2014
CQG. 31 105011

oscillation of the star (e.g. r-modes)

$f \sim 4f_\star/3$

precession multiples harmonics

$\theta \neq 0$

heterogeneous stars (multiple phases of component matter)

$f_1 = 2f_\star, \; f_2 = f_\star$

How the signal looks like

A CW received at the detector is NOT exactly monochromatic

- **SPIN-DOWN (or SPIN-UP)**

  $\dot{f} \propto f^n$ **EM (n~3), GW (n=5), r-mode (n=7)**

- DOPPLER

  $$f(t) = f_0(t)\left(1 + \frac{\vec{v} \cdot \hat{n}}{c}\right)$$ daily+yearly cycle

- **SPIN WANDERING**
- **SIDEREAL VARIATION of the amplitude**

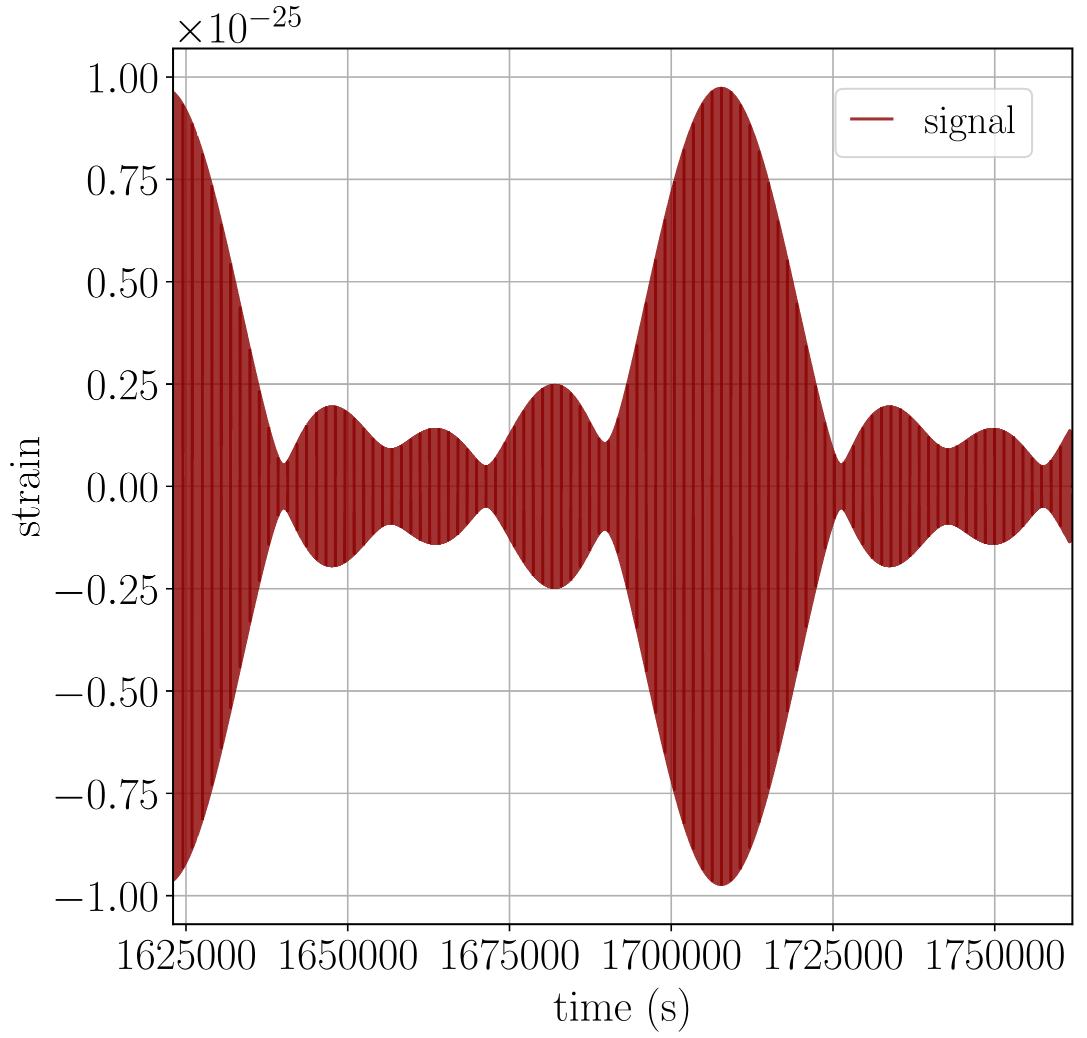

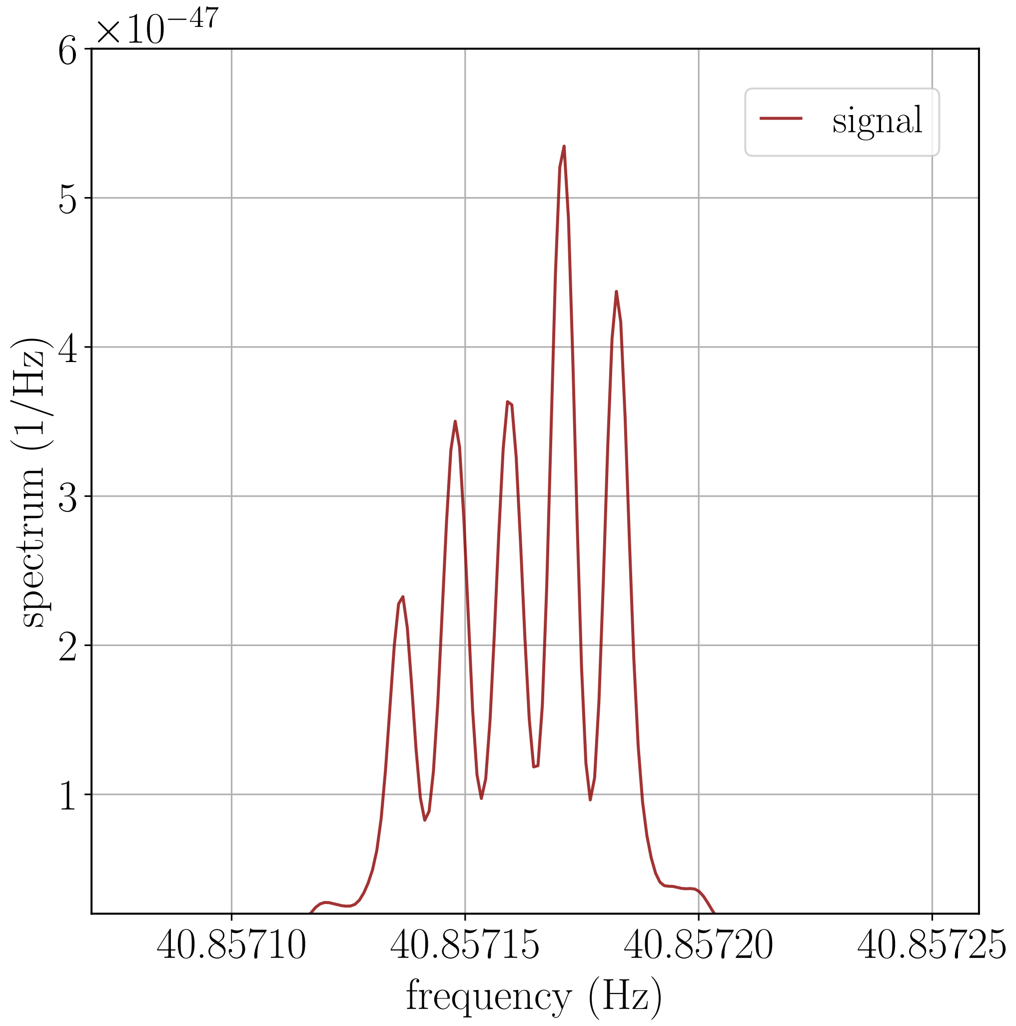

Credit: Karl Wette

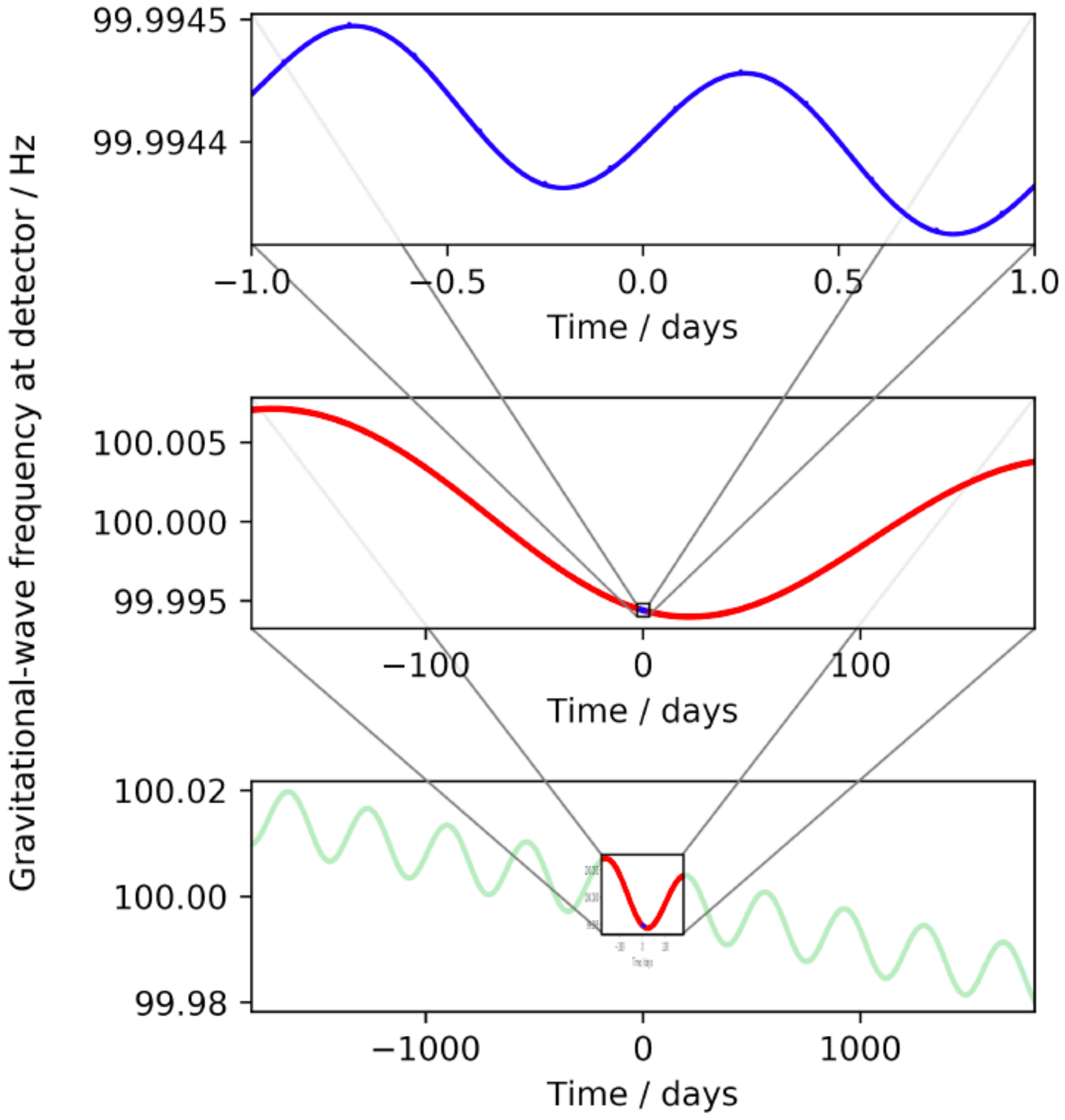

+modulation due to a companion

CW searches

See also **Pep Covas's talk**

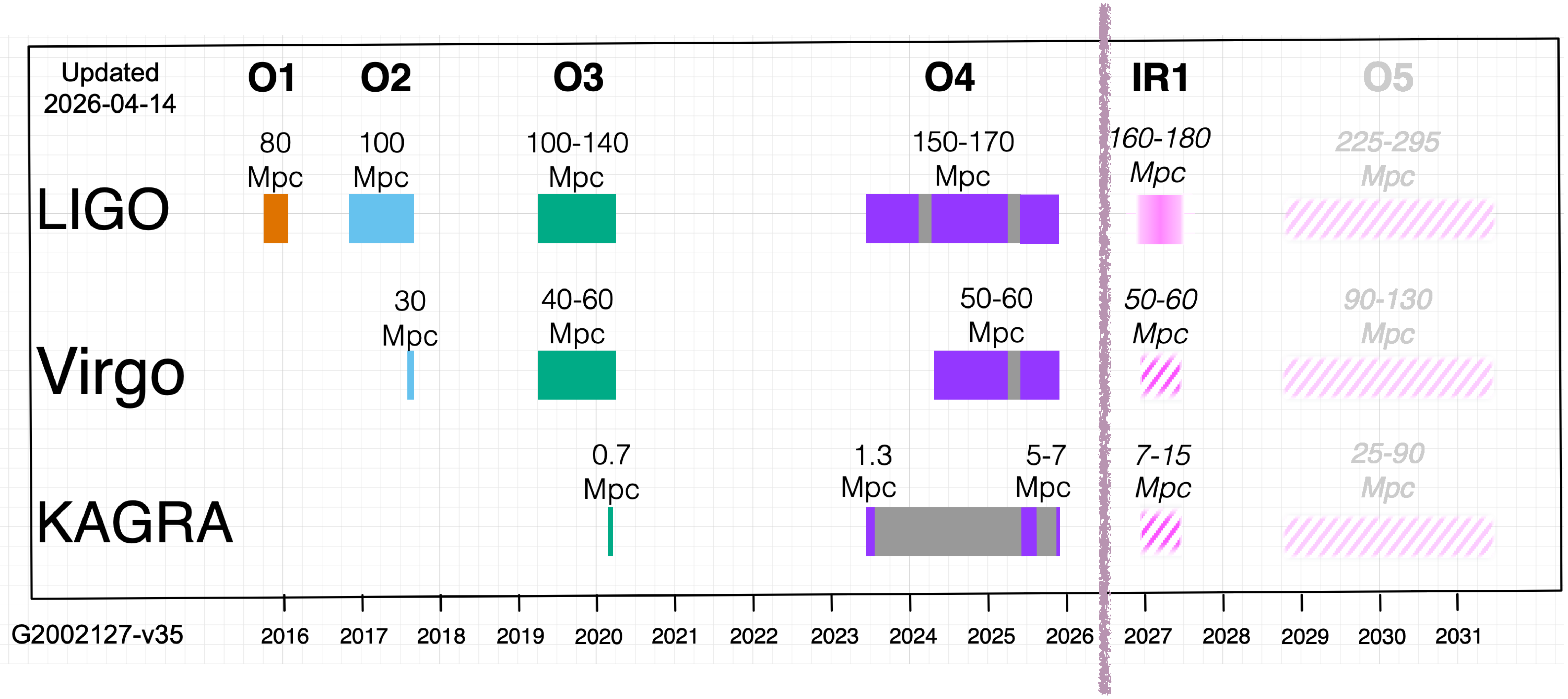

9 papers released and 11 in preparation

Table 2: Data collection runs of the LIGO and Virgo gravitational wave detectors, 2002–2020. Columns are: detector generation, run label, start date, end date, time-span, and number of CW searches reviewed in Sec. 6 which used data from the run. (Some CW searches use data from more than one run, which is accounted for in column 6.)

Gen.	Obs.	Start	End	T days	CW #
0.5G	S1	23 Aug 2002	9 Sep 2002	17	2
0.5G	S2	14 Feb 2003	14 Apr 2003	59	4
0.5G	S3	31 Oct 2003	9 Jan 2004	70	1
0.5G	S4	22 Feb 2005	23 Mar 2005	29	5
1G	S5	4 Nov 2005	1 Oct 2007	696	14
1G	VSR1	18 May 2007	1 Oct 2007	136	1
1.5G	VSR2	7 Jul 2009	8 Jan 2010	185	9
1.5G	S6	7 Jul 2009	20 Oct 2010	470	22
1.5G	VSR3	11 Aug 2010	19 Oct 2010	69	2
1.5G	VSR4	3 Jun 2011	5 Sep 2011	94	6
2G	O1	12 Sep 2015	19 Jan 2016	129	57
2G	O2	30 Nov 2016	25 Aug 2017	268	79
2G	O3	1 Apr 2019	27 Mar 2020	361	116
	– a	1 Apr 2019	1 Oct 2019	183	
	– b	1 Nov 2019	27 Mar 2020	147	

Wette, Astroparticle Physics 153 (2023) 102880

Type of CW searches

The source input parameters $(\alpha, \delta, f_0, \dot{f}_0, \ldots)$ can be provided by the EM community and are fundamental to carry out some of the searches

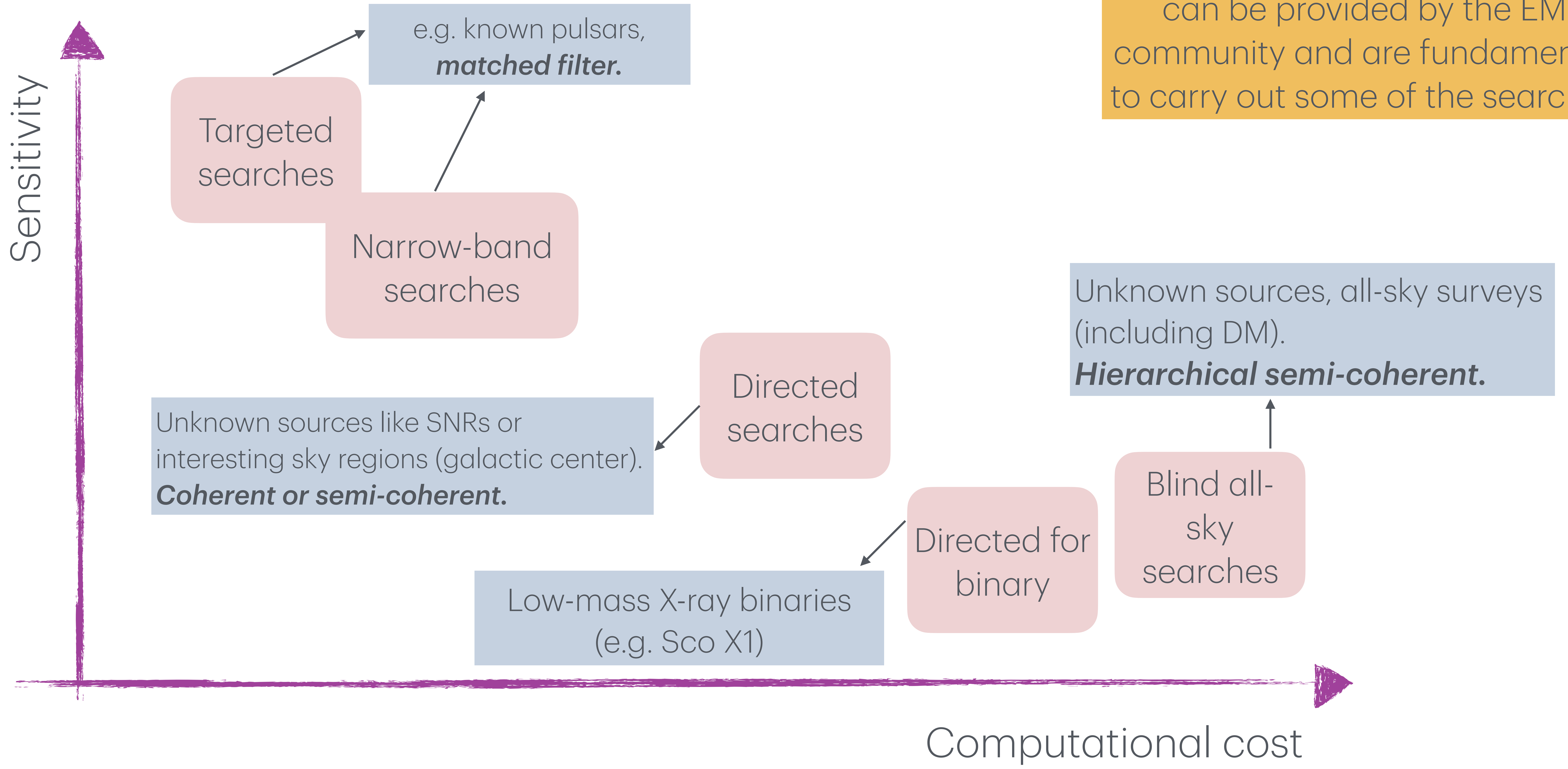

Reviews: Piccinni, Galaxies, 10(3) (2022)

Targeted O4a

- EM data in the gamma, X-rays and radio.
- **45 known pulsars** (11 binaries)
- 3 methods: *time-domain Bayesian; the F/G/D-statistic; 5-vector + narrowband search* (16, 2 glitching)
- Both ***single*** and ***dual harmonic emission*** probed
- Extra polarization test (Brans-Dicke)
- **J0537−6910** which had the **most constraining** amplitude upper limit of **6.38x10^{-27}**

29 out of the 45 pulsars have strain amplitudes lower than the limits calculated from their electromagnetically measured spin-down rates

LVK, Astrophys. J. **983**, 99 (2025)

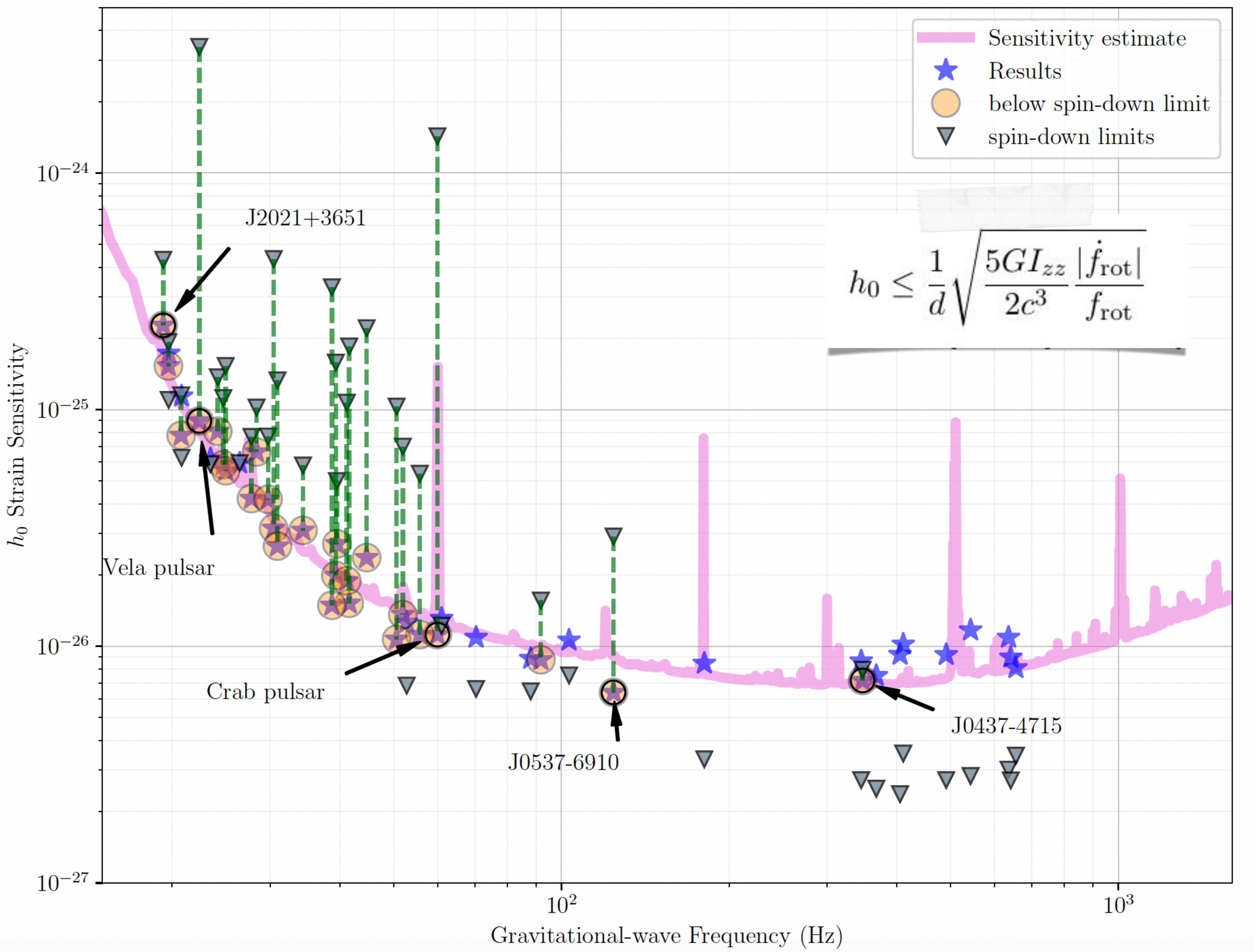

For the Crab and Vela pulsars, these limits are ~130 and ~40 times lower than their spin-down limits

Targeted O4a

- Limits recasted as constraints on equatorial deformations, or **ellipticity**

$$h_0 = \frac{4\pi^2 G}{c^4}\frac{\epsilon I_{zz} f^2}{d}$$

characteristic age $\tau = \frac{P}{4\dot{P}}$

assuming that GW emission alone is causing spin-down.

LVK, Astrophys. J. **983**, 99 (2025)

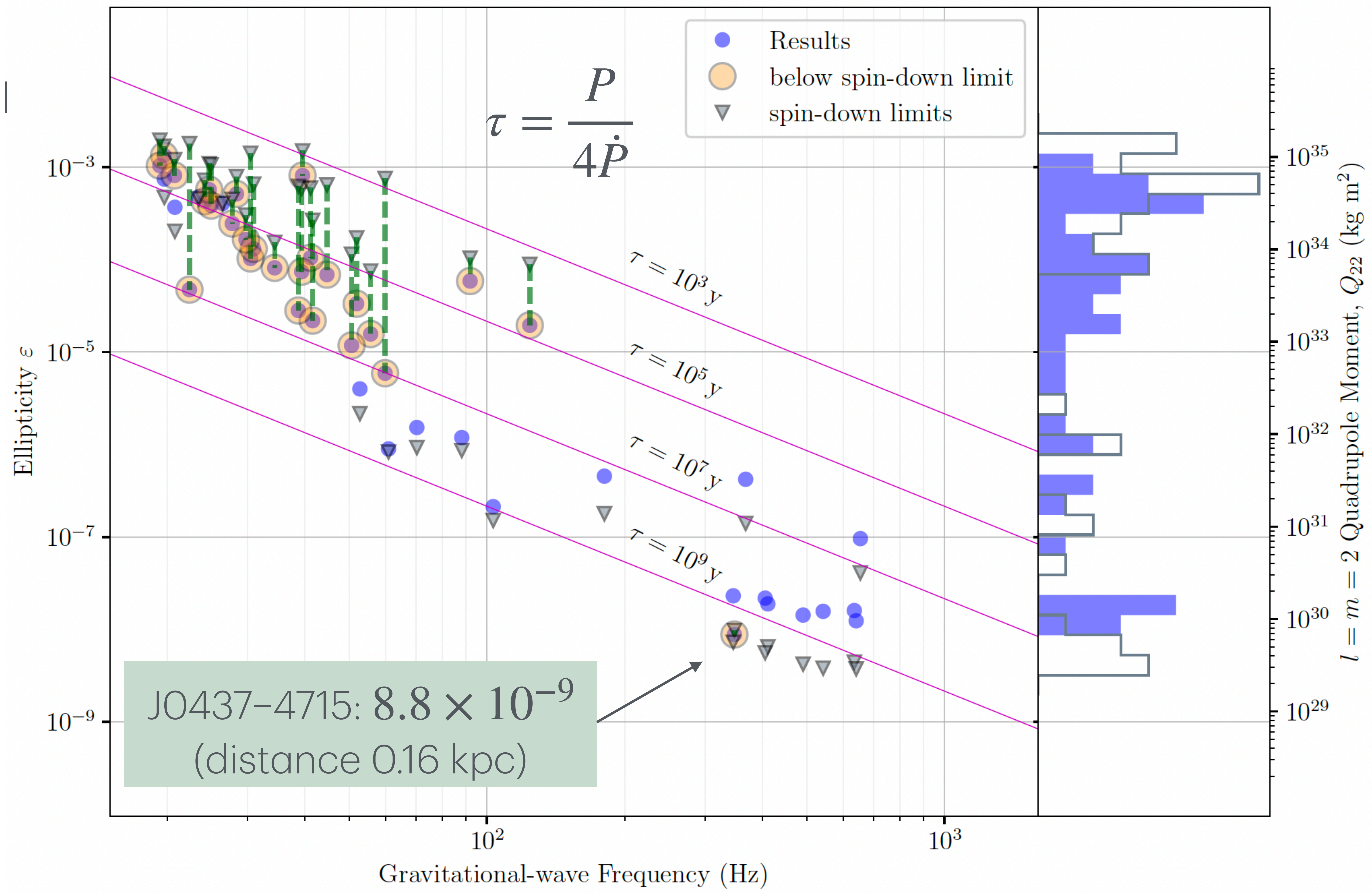

For J0437–4715, we are measuring deformation of less than 100 microns, assuming a neutron star radius of 10 km!

Narrowband O4a+O4b

LVK, arXiv:2603.25938

- EM data in the gamma, X-rays and radio
- **34 known pulsars** (some binaries)
- 1 method: 5-vector narrowband search
- ***dual harmonic emission + $\ddot{f}$***
- First narrowband search including binary pulsars
- No detection; 20 analyses beat spin-down limit
- Limits recasted as **ellipticity** constraints

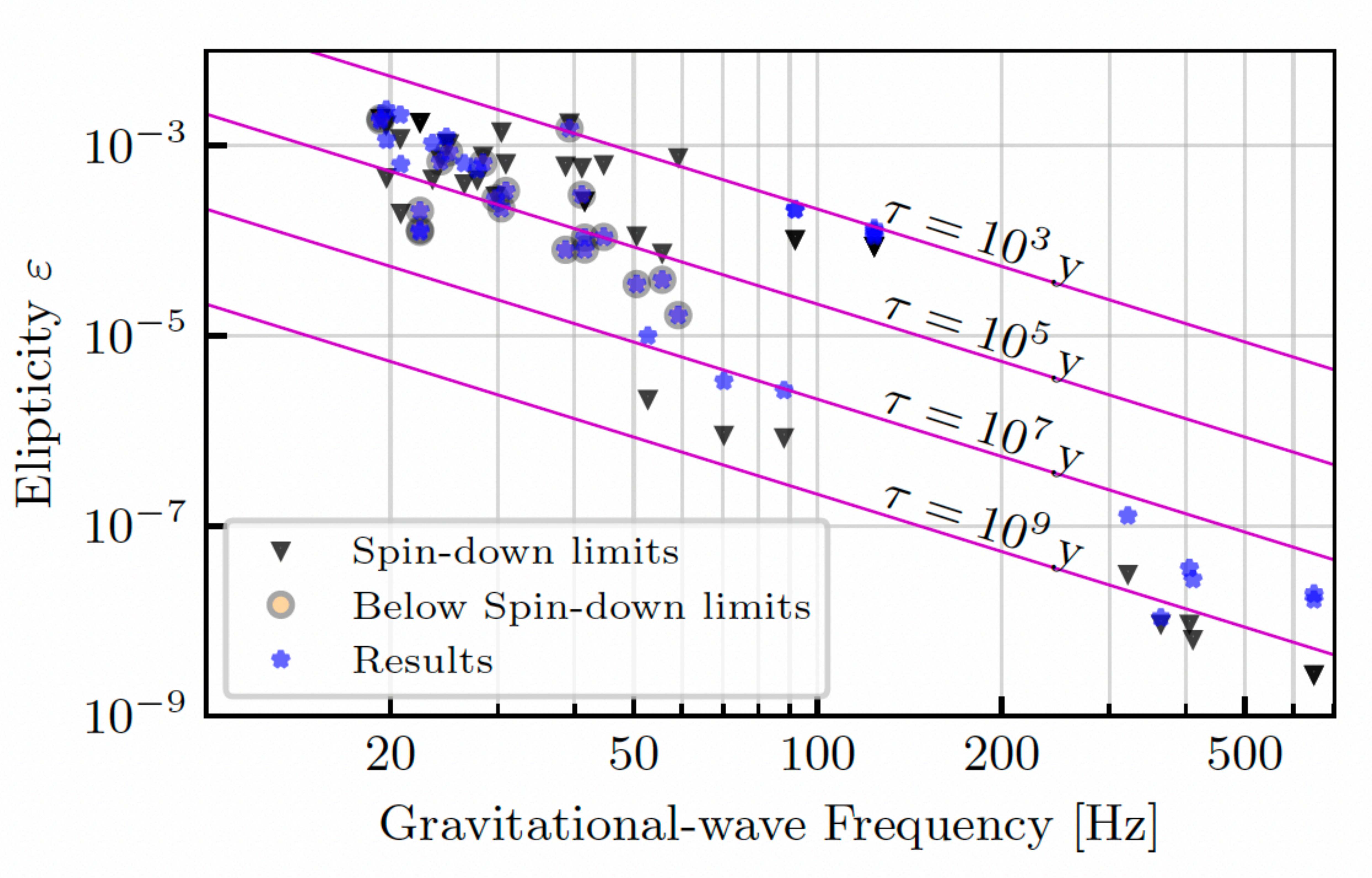

Crab pulsar: strongest result at ~2% of spin-down limit ($h_0^{95\%}/h_0^{sd} \approx 0.02$), less than about 0.04% of spin-down power goes into CW emission

The Vela glitch

- Young, nearby, frequently glitching pulsar (29 Apr 2024, during LIGO O4b); radio timing from IAR and MPRO
- Search both for **seconds-scale burst-like emission** (fundamental f-mode oscillations), and for **longer transients** (fluid motions or transient mountains) up to four months in duration:
- GW energy fractions Q=EGW/Ec≪1, direct GW limits from a real glitch beat the indirect energy budget:
  - Vela-like glitches ***do not typically radiate a large fraction of their energy as GWs*** in either short f-modes or long quadrupolar transients
  - GW non-detections already carve out parts of glitch-emission parameter space

Q=0.017 "transient mountain" Yim&Jones 2020

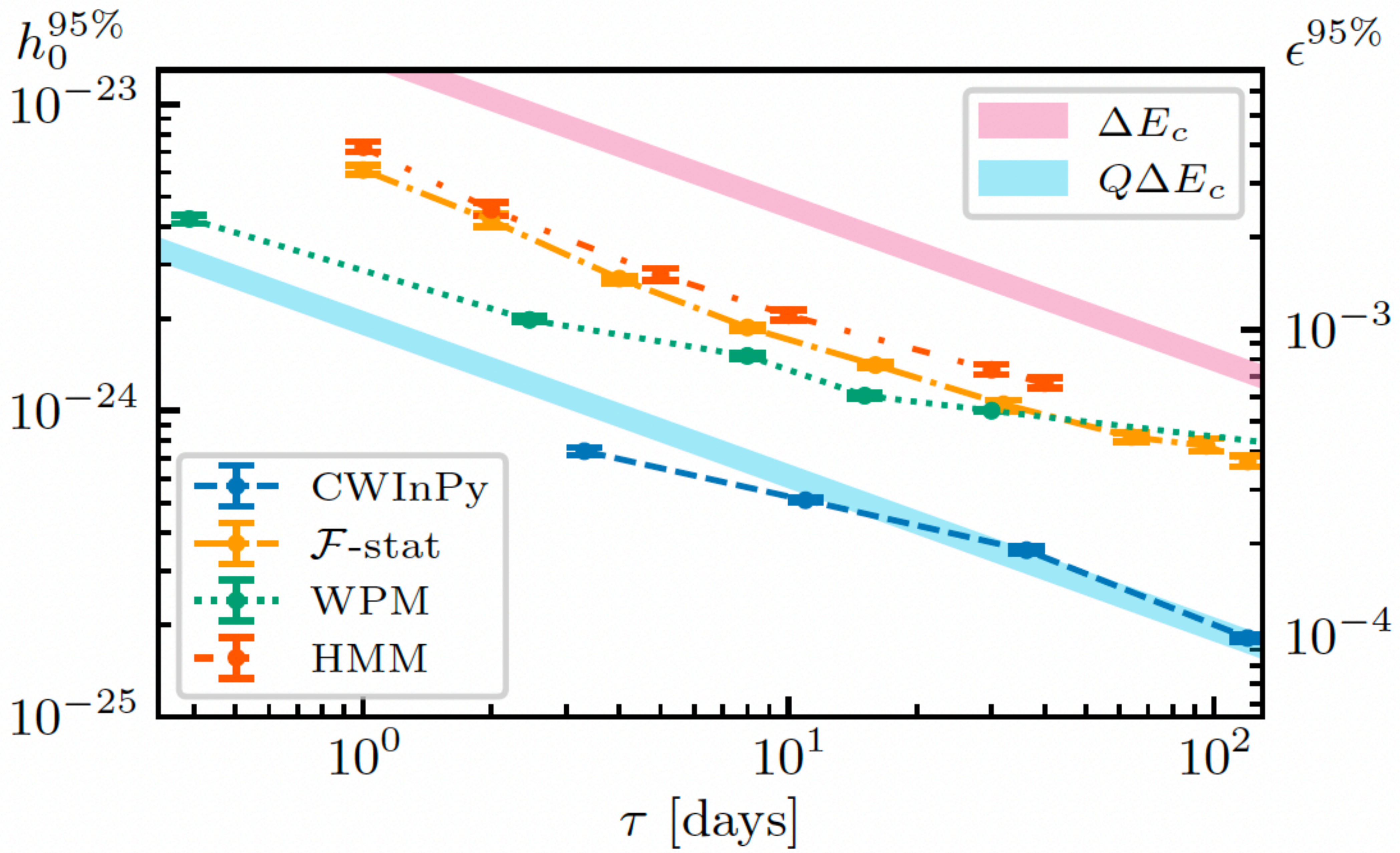

$$h_0^{Q\Delta E_c} \approx \frac{1}{d}\sqrt{\frac{5G}{2c^3}\frac{I}{\tau}Q\frac{\Delta f_{\rm rot}}{f}}$$

LVK arXiv:2512.17990

Supernova remnants O4a

LVK, arXiv:2603.25808 (accepted by ApJ)

- EM data in the gamma, X-rays and radio
- **15 nearby supernova remnants** (likely young NS candidates) including Vela Jr., Cas A and G347.3-0.5, SNR 1987A
- 5 methods: *BSD directed; Weave; Viterbi (SHV+DHV); PyStoch*
- Both single and dual harmonic emission probed
- Wide frequency bands (~10 Hz–2 kHz), no prior ephemerides
- Strain limits recasted as **ellipticity/r-mode** amplitude constraints
- Vela Jr. (G266.2–1.2): most stringent $h_0^{95\%}$ ~$\mathbf{4\times10^{-26}}$ near 300 Hz

Source	Compact Object or PWN association
G1.9+0.3	–
G15.9+0.2	CCO CXOU J181852.0−150213
G18.9−1.1 G18.9-1.1 G18.9−1.1	PWN, CXOU J182913.1−125113
G39.2−0.3/3C 396	PWN, CXOU J190404.7+052711.8
G65.7+1.2/DA 495	PWN, CXO J195217.04 +292552.5
G93.3+6.9/DA 530	PWN candidate, CXOU J205214+551722
G111.7−2.1/Cas A	CCO CXOUJ232327.9+584842
G189.1+3.0/IC 443	PWN G189.23+2.90
G266.2−1.2/Vela Jr.	CCO CXOU J085201.4−461753
G291.0−0.1/MSH 11–62	PWN G291.02−0.11, CXOU J111148.6−603926
G330.2+1.0	CCO CXOU J160103.1−513353
G347.3−0.5/RX J1713.7-3946	CCO 1WGA J1713.4-3949
G350.1−0.3	CCO candidate XMMU J172054.5-372652
G353.6−0.7	CCO XMMU J173203.3-344518
G279.7−31.9/SNR 1987A	NS or PWN

Supernova remnants O4a

$$\epsilon = 9.5 \times 10^{-5} \left(\frac{h_0}{10^{-24}}\right)\left(\frac{d}{1\mathrm{kpc}}\right)\left(\frac{100\ \mathrm{Hz}}{f}\right)^2$$

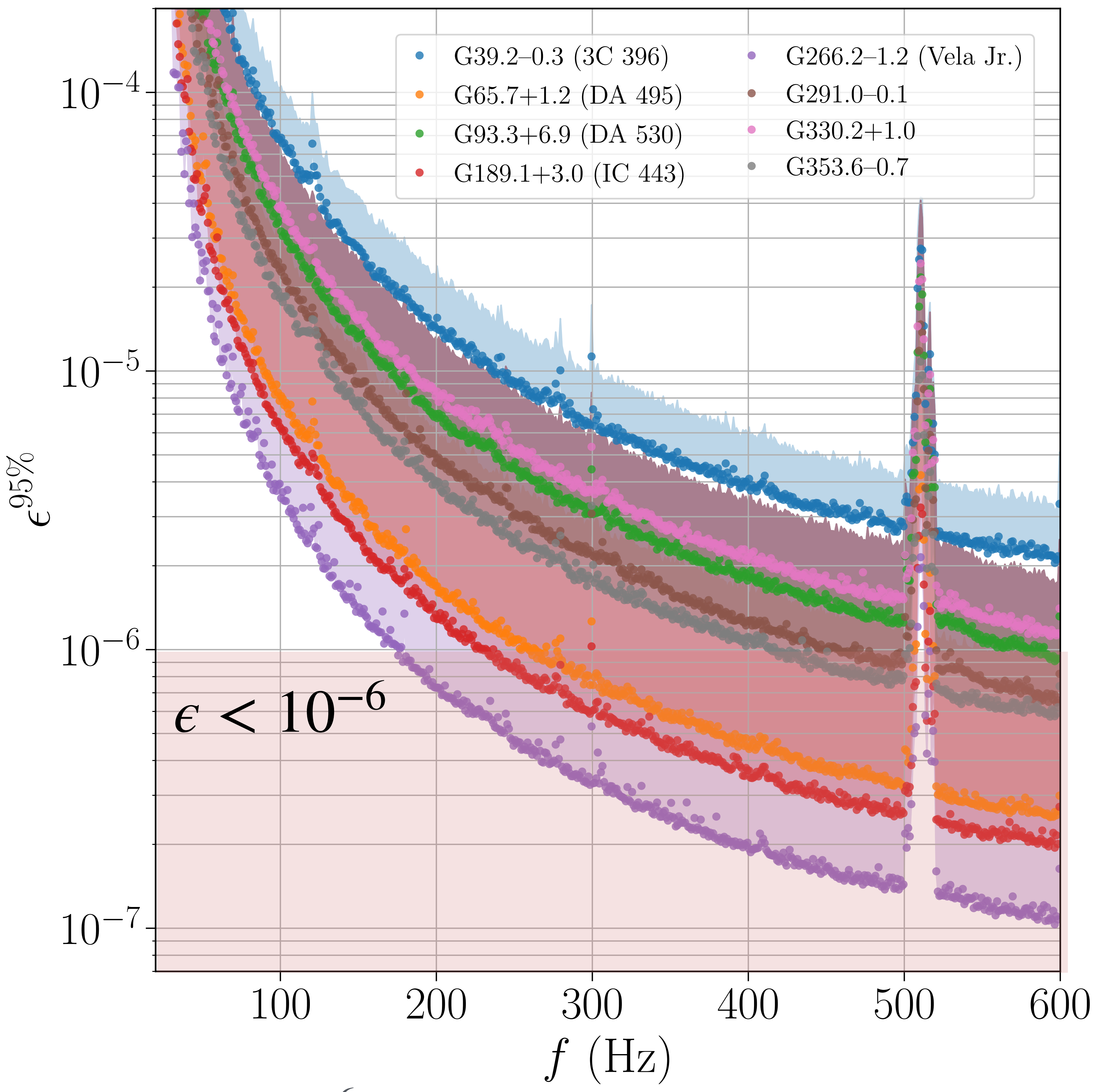

$$\alpha \simeq 0.028 \left(\frac{h_0}{10^{-24}}\right)\left(\frac{d}{1\mathrm{kpc}}\right)\left(\frac{100\ \mathrm{Hz}}{f}\right)^3$$

$M = 1.4 M_\odot, R = 11.7$ km

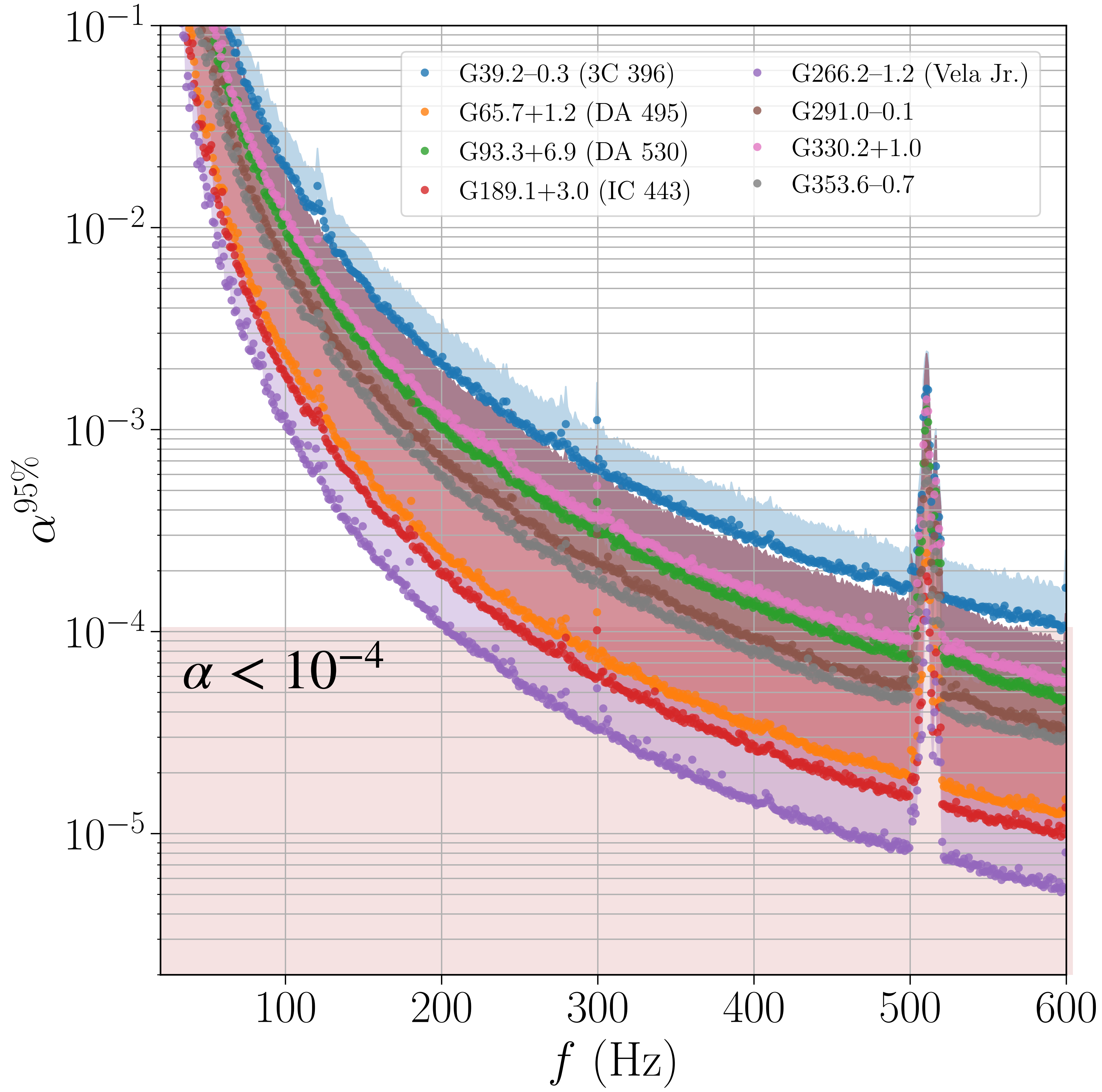

- Ellipticity $\epsilon < 10^{-6}$ for most of the sources; less than theoretical limits for normal neutron stars (Johnson-McDaniel & Owen 2013),
- r-mode amplitude $\alpha < 10^{-4}$, reaching below the theoretical prediction expected for the nonlinear saturation mechanisms (Bondarescu et al. 2009)

All-sky isolated O4a

LVK, arXiv:2603.14168

- ***No EM information needed***, search over the full sky
- 3 methods: *PowerFlux, BSD-Frequency Hough, SOAP*
- Frequency **20–2000 Hz, wide spin-down range up to ~10^{-8} Hz/s**
- Both single and dual harmonic emission probed
- Stringent population-averaged upper limits **9.7×10^{-26}**
- **Strain limits improved ~30% over O3**
- Limits interpreted for ***Galactic NS population***, Galactic-center ***MSP GeV excess***, and asteroid-mass ***PBH binaries***

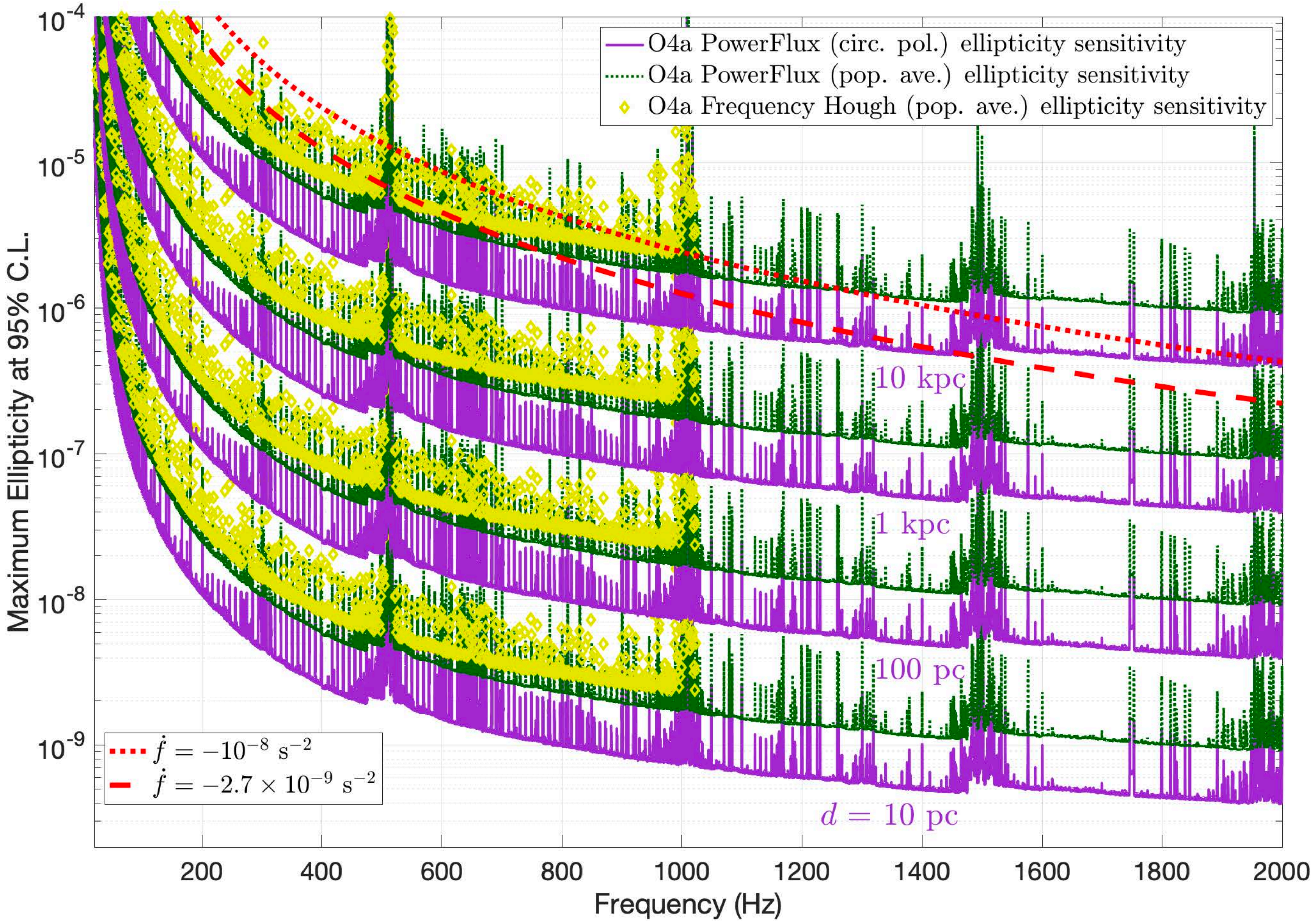

All-sky search for binaries

LVK, arXiv:2511.16863

- Several NSs expected to be in **binary systems**
- Parameter space: *7-15 days orbital period* in the *100-350 Hz* band; covering parameter of **closeby known pulsars** in binaries
- New method: GPU-accelerated *FastTracks + Hough transform*
- More than **10^{16} templates** used
- Additional Doppler modulation due to the source motion in the binary
- Robust against small deviations from zero-eccentricity and zero-spin down/up systems
- Sensitivity **improvement of 1.5 compared to O3a** (1.62 x 10^{-25}) at ~200 Hz

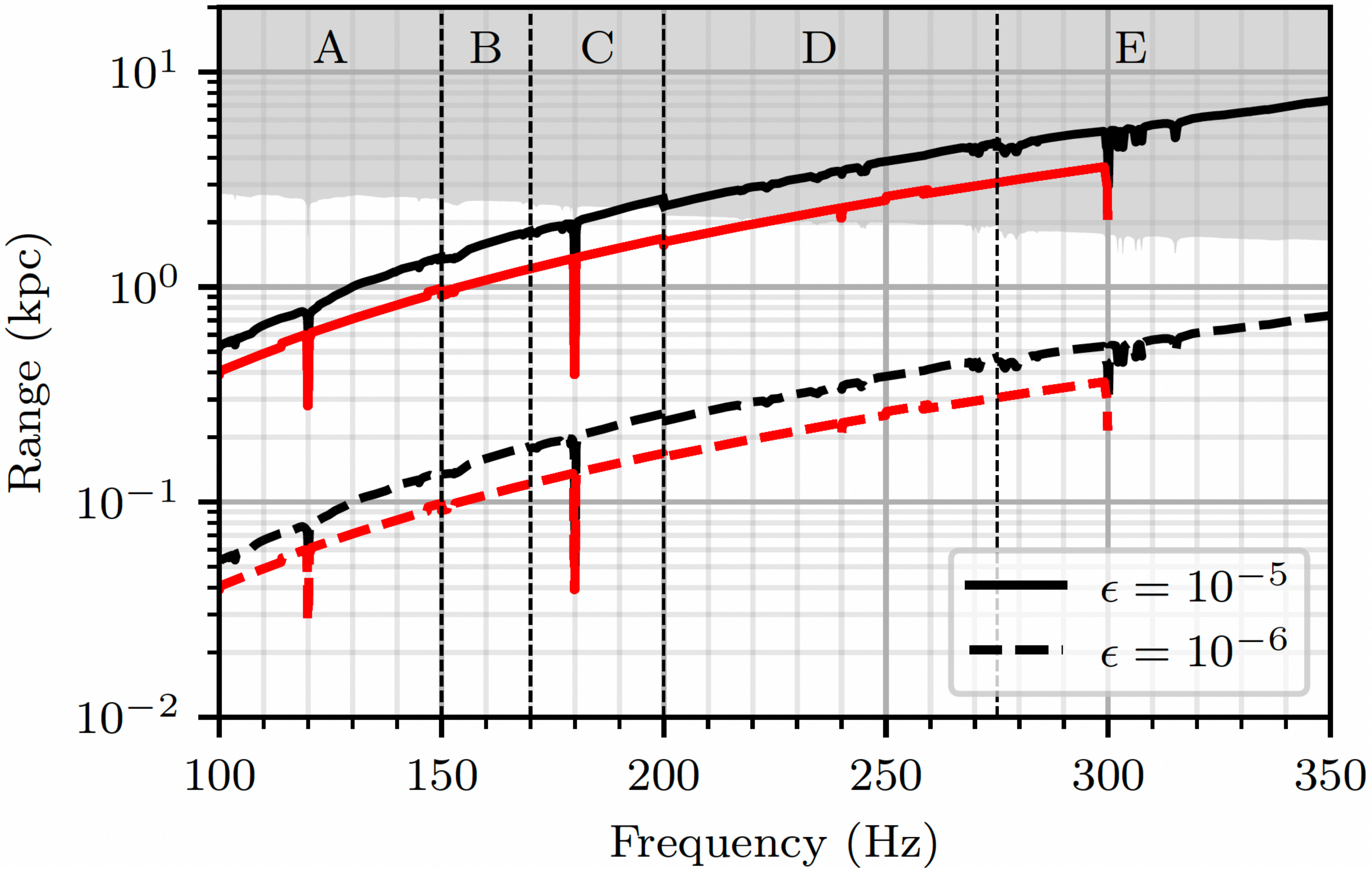

Stringent limits yet on CW signals from unknown neutron stars in binary systems (see Pep's talk)

The "inverse problem"

What can a detection tell us about the source?

See Lu+ (2023)
Jones&Riles arXiv:2403.02066
Sieniawska&Jones (2022)
Sieniawska+ (2023)

- First step is to identify mechanism:
  - If spin is known: $f_{\mathrm{GW}} \approx 2f_{\mathrm{spin}} \rightarrow$ mountain; $f_{\mathrm{GW}} \approx \frac{4}{3} f_{\mathrm{spin}} \rightarrow$ r-mode (idealized, Newtonian)
  - In special cases, braking index $n = f_{\mathrm{GW}} \ddot{f}_{\mathrm{GW}} / \dot{f}^2_{\mathrm{GW}}$ can discriminate r-mode (n ≈ 7) vs mountain (n ≈ 5), but this is observationally demanding.

- **r-modes**:
  - Deviations of $f_{\mathrm{GW}} / f_{\mathrm{spin}}$ from 4/3 (GR corrections) encode ***compactness M/R*** and thus EOS.
  - Detections and non-detections map the r-mode instability window in spin–temperature space, constraining the combined ***dissipation mechanisms*** (superfluidity, viscosities, etc.).

The "inverse problem"

What can a detection tell us about the source?

See Lu+ (2023)
Jones&Riles arXiv:2403.02066
Sieniawska&Jones (2022)
Sieniawska+ (2023)

- **Mountains**:
  - From non-detections (known spin + distance) → ***upper limits on ellipticity.***
  - Assuming elastic mountains → ***constrain actual crustal strain***, but typical values are uncertain.
  - Assuming magnetic mountains → ***constrain internal magnetic field;*** comparisons with external dipole field can rule out the magnetic or elastic origin.
  - Even with a detection, ***CW data alone cannot uniquely distinguish elastic vs magnetic mountains***; extra astrophysical information is needed.

With a joint CW and EM observation we may know: NS radius, mass, magnetic field and ellipticity... (EOS inference)

Bonus: we can, in principle, follow the signal indefinitely

What's next

Prospect of detection with ET

- Studies show that we can ***reach the edges of the galaxies*** for sources emitting at frequencies above 200 Hz and ellipticities bigger than 10^{-6}
- For ellipticities of the order of **10^{-8}**, ET can detect galactic sources at a distance from ~100 pc to 10 kpc, frequencies above 200 Hz

Configuration	n_1 ($\epsilon_{\rm med}$)	n_2 ($\epsilon_{\rm med}$)	n_3 ($\epsilon_{\rm med}$)
Δ 10km	866 (1.3×10^{-4})	180 (4.4×10^{-9})	19 (7.5×10^{-10})
2L 15km	959 (1.2×10^{-4})	206 (4.2×10^{-9})	29 (8.1×10^{-10})

Spin-down limit, 10^{-6}, 10^{-9}

distance reach for different ellipticities

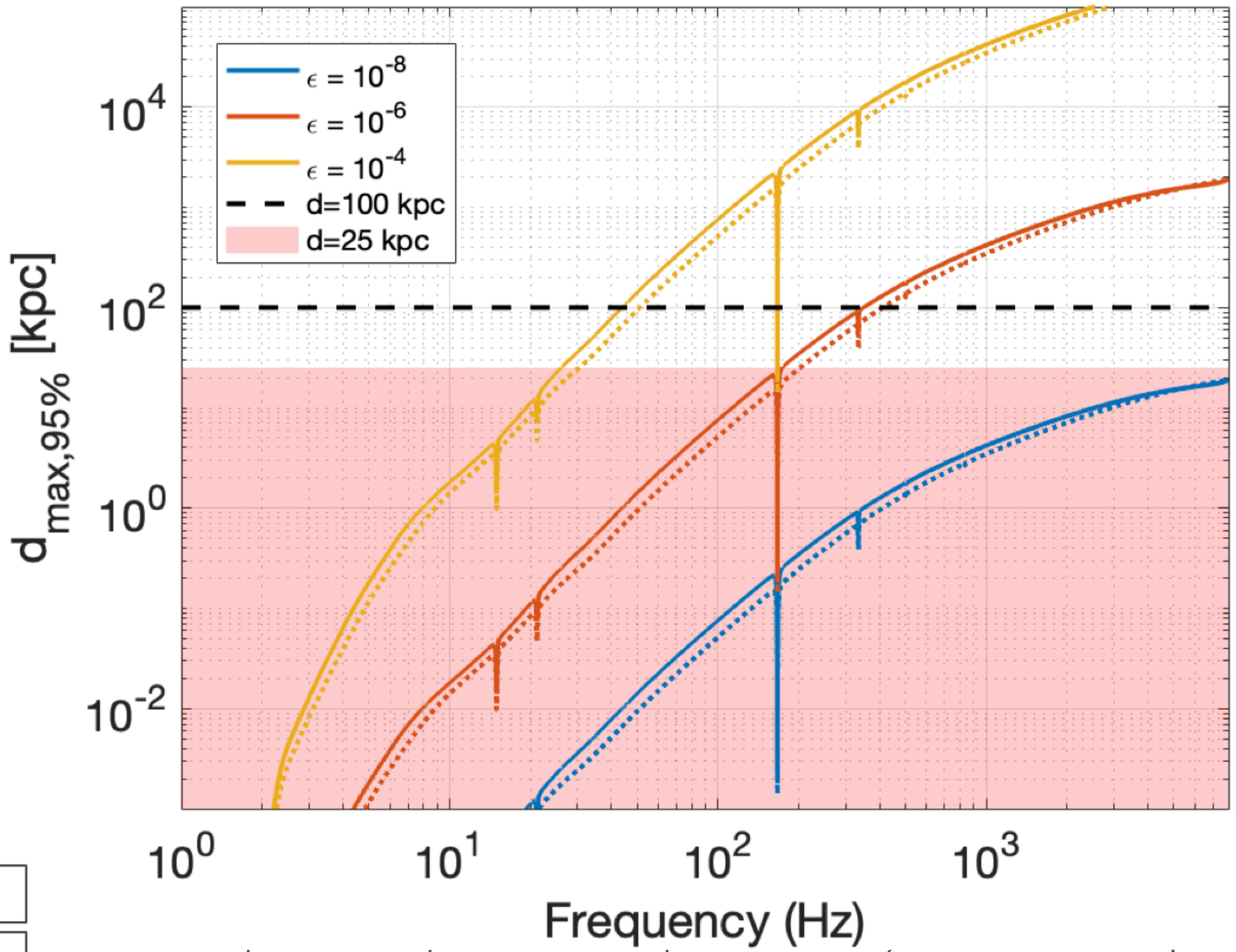

L-shape 15km arms detectors (continuous lines)
triangular 10 km arms detector (dashed lines)
Abac+ arXiv:2503.12263 (2026)

Conclusion

- **CW could be the next surprise in GW astronomy given the enhanced sensitivity of the detectors, noise characterization is fundamental; efforts ongoing to increase the sensitivity of the pipelines.**

- **For the standard NS case scenario, we are probing very low ellipticities in a physically realistic regime**

- **Exciting times especially if a joint CW and EM observation occurs (constraints on NS interior), remarking the importance of MMA**

- **Searches for long-lasting signals are still ongoing for O4**

- **We expect (and hope) to find several surprises in O4!**

Acknowledgments

This material is based upon work supported by NSF's LIGO Laboratory which is a major facility fully funded by the National Science Foundation. LIGO Laboratory and Advanced LIGO are funded by the United States National Science Foundation (NSF) as well as the Science and Technology Facilities Council (STFC) of the United Kingdom, the Max-Planck-Society (MPS), and the State of Niedersachsen/Germany for support of the construction of Advanced LIGO and construction and operation of the GEO600 detector. Additional support for Advanced LIGO was provided by the Australian Research Council. Virgo is funded, through the European Gravitational Observatory (EGO), by the French Centre National de Recherche Scientifique (CNRS), the Italian Istituto Nazionale di Fisica Nucleare (INFN) and the Dutch Nikhef, with contributions by institutions from Belgium, Germany, Greece, Hungary, Ireland, Japan, Monaco, Poland, Portugal, Spain. KAGRA is supported by Ministry of Education, Culture, Sports, Science and Technology (MEXT), Japan Society for the Promotion of Science (JSPS) in Japan; National Research Foundation (NRF) and Ministry of Science and ICT (MSIT) in Korea; Academia Sinica (AS) and National Science and Technology Council (NSTC) in Taiwan.

O.J.P. is supported by the Spanish Ministerio de Ciencia, Innovacion y Universidades Ramon y Cajal, RYC2023-044489-I funded by MCIN/AEI/ 10.13039 /501100011033 and the FSE+ and cofinanced by the Universitat de les Illes Balears (UIB). This work was supported by UIB with funds from the Programa de Foment de la Recerca i la Innovació de la UIB 2024-2026 (supported by the yearly plan of the Tourist Stay Tax ITS2023-086); the Spanish Agencia Estatal de Investigación grants RED2024-153978-E, RED2024-153735-E, funded by MICIU/AEI/10.13039/501100011033 and the ERDF/EU; and the Comunitat Autònoma de les Illes Balears through the Conselleria d'Educació i Universitats with funds from the ERDF (SINCO2022/18146)